J|A|C|S
ARTICLES
Published on Web 08/22/2006

Investigation of Two-Photon Absorption Properties in Branched Alkene and Alkyne Chromophores

Ajit Bhaskar,[†] Guda Ramakrishna,[†] Zhikuan Lu,[‡] Robert Twieg,[‡] Joel M. Hales,[§] David J. Hagan,[§] Eric Van Stryland,[§] and Theodore Goodson III*,[†]

Contribution from the Departments of Chemistry and Macromolecular Science and Engineering, University of Michigan, Ann Arbor, Michigan 48109, Department of Chemistry, Kent State University, Kent, Ohio 44242, and School of Optics/CREOL, University of Central Florida, Orlando, Florida 32816

Received January 26, 2006; E-mail: tgoodson@umich.edu

Abstract: Novel alkene and alkyne branched structures have been synthesized, and their two-photon absorption (2PA) properties are reported. This series of alkene and alkyne trimer systems tests the mechanistic approach for enhancing the 2PA process which is usually dictated by the π-bridging, delocalization length, and corresponding charge transfer on the 2PA cross sections. The results suggest that alkene branched systems have higher 2PA cross sections. While steady-state absorption and emission measurements were not successful in predicting the observed trend of 2PA cross sections, time-resolved measurements have explained the trends observed. It was found that, upon photoexcitation, there is an ultrafast charge localization to an intramolecular charge-transfer (ICT) state, followed by the presence of a solvent and conformationally relaxed ICT state ′ in these branched systems.

1. Introduction

The development of conjugated organic molecules with large two-photon absorption (2PA) cross sections[1] is of broad interest in many areas of research. Much of the interest is driven by potential applications in 3D microfabrication,[2−5] photodynamic therapy,[6] two-photon microscopy,[7−10] optical power limiting,[11,12] and optical data storage.[13−15] To realize these applications, novel molecules with large 2PA cross sections in the visible, near-infrared, and telecommunication wavelengths are desired. Several design approaches have been reported for the synthesis of organic molecules with large 2PA cross sections. Molecules with dipolar and quadrupolar character have been the focus of development.[16−28] Numerous dipolar chromophores have been synthesized with varying donor−π−acceptor configurations, as well as different π-bridging centers, and different donor−acceptor strengths so as to probe the structure and 2PA property relationships.[1,20,22] Recent investigations indicate that increasing the dimensionality of donor−π−acceptor molecules is a good approach, as certain branched systems exhibit enhanced 2PA cross sections over the linear counterparts.[29,30] This is believed to be a consequence of cooperative interaction among the

[†] University of Michigan.
[‡] Kent State University.
[§] University of Central Florida.

(1) (a) Cumpston, B. H.; et al. *Nature* **1999**, *398*, 51. (b) Albota, M.; et al. *Science* **1998**, *281*, 1653.
(2) Zhou, W.; Kuebler, S. M.; Braun, K. L.; Yu, T.; Cammack, J. K.; Ober, C. K.; Perry, J. W.; Marder, S. R. *Science* **2002**, *296*, 1106.
(3) Kawata, S.; Sun, H.-B.; Tanaka, T.; Takada, K. *Nature* **2001**, *412*, 697.
(4) Sun, H.-B.; Mizeikis, V.; Xu, Y.; Juodkazis, S.; Ye, J.-Y.; Matsuo, S.; Misawa, H. *Appl. Phys. Lett.* **2001**, *79*, 1.
(5) Maruo, S.; Nakamura, O.; Kawata, S. *Opt. Lett.* **1997**, *22*, 132.
(6) Denk, W.; Strickler, J. H.; Webb, W. W. *Science* **1990**, *248*, 73.
(7) Bhawalkar, J. D.; Kumar, N. D.; Zhao, C. F.; Prasad, P. N. *J. Clin. Laser Med. Surg.* **1997**, *15*, 201.
(8) He, G. S.; Markowicz, P. P.; Line, P.-C. Prasad, P. N. *Nature* **1999**, *415*, 767.
(9) Xu, C.; Zipfel, W.; Shear, J. B.; Williams, R. M.; Webb, W. W. *Proc. Natl. Acad. Sci. U.S.A.* **1996**, *93*, 10763.
(10) Larson, D. R.; Zipfel, W. R.; Williams, R. M.; Clark, S. W.; Bruchez, M. P.; Wise, F. W.; Webb, W. W. *Science* **2003**, *300*, 1434.
(11) He, G. S.; Xu, G. C.; Prasad, P. N.; Reinhardt, B. A.; Bhatt, J. C.; McKellar, R.; Dillard, A. G. *Opt. Lett.* **1995**, *20*, 435.
(12) Calvete, M.; Yang, G. Y.; Hanack, M. *Synth. Met.* **2004**, *141*, 231.
(13) Parthenopoulos, D. A.; Rentzepis, P. M. *Science* **1989**, *245*, 843.
(14) Strickler, J. H.; Webb, W. W. *Opt. Lett.* **1991**, *16*, 1780.
(15) Belfield, K. D.; Schafer, K. J. *Chem. Mater.* **2002**, *14*, 3656.
(16) Marder, S. R.; Beratan, D. N.; Cheng, L. T. *Science* **1991**, *252*, 103.
(17) Kanis, D. R.; Ratner, M. A.; Marks, T. J. *Chem. Rev.* **1994**, *94*, 195.
(18) Brédas, J.-L.; Cornil, K.; Meyers, F.; Beljonne, D. In *Handbook of Conducting Polymers*; Skotheim, T. A., Elsenbaumer, R. L., Reynolds, J. R., Eds.; Marcel Dekker: New York, 1998.
(19) He, G. S.; Yuan, L.; Cheng, N.; Bhawalkar, J. D.; Prasad, P. N.; Brott, L. L.; Clarson, S. J.; Reinhardt, B. A. *J. Opt. Soc. Am. B* **1997**, *14*, 1079.
(20) Ehrlich, J. B.; Wu, X. L.; Lee, I.-Y. S.; Hu, Z.-Y.; Rockel, H.; Marder, S. R.; Perry, J. W. *Opt. Lett.* **1997**, *22*, 1843.
(21) He, G. S.; Gvishi, R.; Prasad, P. N.; Reinhardt, B. A. *Opt. Commun.* **1995**, *117*, 133.
(22) (a) Kim, O. K.; Lee, K. W.; Woo, H. Y.; Kim, K. S.; He, G. S.; Swiatkiewicz, J.; Prasad, P. N. *Chem. Mater.* **2000**, *12*, 284. (b) Kannan, R.; Chung, S.; Lin, T.; Prasad, P. N.; Vaia, R. A.; Tan, L. *Chem. Mater.* **2004**, *16*, 185.
(23) Reinhardt, B. A.; Brott, L. L.; Clarson, S. J.; Dillard, A. G.; Bhatt, J. C.; Kannan, R.; Yuan, L.; He, G. S.; Prasad, P. N. *Chem. Mater.* **1998**, *10*, 1863.
(24) Strehmel, B.; Sarker, A. M.; Detert, H. *ChemPhysChem* **2003**, *4*, 249.
(25) Zojer, E.; Beljonne, D.; Kogej, T.; Vogel, H.; Marder, S. R.; Perry, J. W.; Bredas, J. L. *J. Chem. Phys.* **2002**, *116*, 3646.
(26) He, G. S.; Lin, T.-C.; Prasad, P. N.; Kannan, R.; Vaia, R. A.; Tan, L.-S. *J. Phys. Chem. B* **2002**, *106*, 11081.
(27) Rumi, M.; Ehrlich, J. E.; Heikal, A. A.; Perry, J. W.; Barlow, S.; Hu, Z. Y.; McCord-Maughon, D.; Parker, T. C.; Rockel, H.; Thayumanavan, S.; Marder, S. R.; Beljonne, D.; Bredas, J. L. *J. Am. Chem. Soc.* **2000**, *122*, 9500.
(28) Pond, S. J. K.; Rumi, M.; Levin, M. D.; Parker, T. C.; Beljonne, D.; Day, M. W.; Bredas, J. L.; Marder, S. R.; Perry, J. W. *J. Phys. Chem. A* **2002**, *106*, 11470.
(29) Beljonne, D.; Wenseleers, W.; Zojer, E.; Shuai, Z.; Vogel, H.; Pond, S. J. K.; Perry, J. W.; Marder, S. R.; Bredas, J.-L. *Adv. Funct. Mater.* **2002**, *12*, 631.

 10.1021/ja060630m CCC: $33.50

individual arms.[30] The interest in multiply branched systems for 2PA also stems from the fact that relatively large 2PA cross sections may primarily be realized from low-lying excited states. Consequently, considerable research has been carried out toward the design and synthesis of multiply branched chromophores. Several configurations, such as donor−π−acceptor, acceptor−π−donor, and chromophores with different branching centers, π-bridging units, and tri- and tetra-branched structures, have been synthesized and studied.[29−50]

Mechanistic investigations aimed at understanding the factors that influence the magnitude of the 2PA cross section in multiply branched systems suggest that it is a complex interplay between intra-arm coupling, electronic delocalization, and extent of intramolecular charge transfer.[37−44] Beljonne et al.[29] have suggested that, within the exciton picture, the 2PA cross section in octupolar molecules should scale by a factor of 3 in comparison to the dipolar counterparts by virtue of increased charge transfer among the three arms. Cho et al.[50] have shown theoretically that, in branched molecules, the 2PA cross section increases as the strength of the donor−acceptor interaction increases. Among several branching centers investigated in octupolar systems, triphenylamine systems were found to show better enhancement of 2PA cross sections with increased branching.[29−32] Prasad and co-workers[30] have shown a 7-fold enhancement of 2PA cross section for trimer (PRL series) over monomer in a triphenylamine-core branched molecule. Macak et al.[49] suggested that electronic coupling is nominal between the arms and vibronic coupling between the arms is significant in enhancing the 2PA of the PRL series of dyes. Mechanistic investigations on the same series of dye molecules suggested that effective electronic delocalization[44] and increased intramolecular charge transfer are possible reasons behind the enhanced 2PA cross section. Also, several triphenylamine-core branched molecules have been synthesized with varying donor−acceptor strength, substituents, and conjugation length.[30−33]

Though larger donor−acceptor strength is important for higher 2PA cross section, the nature and length of the π-linker do play a decisive roles in increasing the 2PA cross section and nonlinear optical (NLO) properties. It has been shown in dipolar chromophores that richer π-electron systems improve the intramolecular charge-transfer character and thereby enhance the NLO properties.[51] Several π-bridging chromophores have been considered for improving the 2PA cross section. Among them, alkene π-bridging is most widely studied, and it has been suggested that, in many of the linear systems, alkene π-bridging is better than alkyne π-bridging.[52,53] However, for several reasons pertaining to intra-arm electronic coupling, charge delocalization, and charge transfer, the consequences of π-bridging on NLO and 2PA properties in branched systems may be different from those in the linear quadrupolar molecules.[54−56] It has been theoretically predicted from ab initio calculations that the 2PA cross sections of alkyne π-bridge-containing quadrupolar molecules are not significantly different from those of their alkene π-bridged analogues.[56,57] However, a systematic experimental study of 2PA in branched trimers with different π-bridging and the underlying mechanism has not been reported.

To understand the effect of π-bridging, acceptor strength, and conjugation length on 2PA cross sections of multiply branched chromophores, we have synthesized new triphenylamine-core branched molecules with pyridine as acceptor (molecules **A**−**D**, Figure 1). Two-photon absorption cross sections of these molecules have been measured by two-photon excited fluorescence and non-degenerate pump−probe techniques. Comparisons of 2PA cross sections were also made with *N*,*N*,*N*-tris[4-{2-(4-{5-[4-(*tert*-butyl)phenyl]-1,3,4-oxadiazol-2-yl}phenyl)-1-ethenyl}phenyl]amine (**PRL-701**) and tris[4-(3′,5′-di-*tert*-butyldistyrylbenzenyl)phenyl]amine ($N(DSB)_3$). Here, we have varied the nature of π-bridging from alkenes (**A** and **C**) to alkynes (**B** and **D**), conjugation length within individual branches (**A** to **B**, **C** to **D**), and acceptor strength at the end of each branch (**B**, PRL-701, and $N(DSB)_3$). Steady-state and time-resolved spectroscopic techniques are employed to probe the mechanism of 2PA. We have correlated the observed 2PA cross sections with the extent of intramolecular charge transfer probed by femtosecond transient absorption spectroscopy. The results of 2PA measurements have shown that alkene π-bridged chromophores have superior 2PA properties over the alkyne π-bridged counterparts at low energy, and we were able to successfully correlate the observed trend with the results of transient absorption spectroscopy. Further, an increase in acceptor group strength as well as an increase in conjugation length within a branch was found to increase 2PA cross sections.

(30) Chung, S.-J.; Kim, K.-S.; Lin, T.-C.; He, G. S.; Swiatkiewicz, J.; Prasad, P. N. *J. Phys. Chem. B* **1999**, *103*, 10741.
(31) Porres, L.; Mongin, O.; Katan, C.; Charlot, M.; Pons, T.; Mertz, J.; Blanchard-Desce, M. *Org. Lett.* **2004**, *6*, 47.
(32) (a) Mongin, O.; Porres, L.; Katan, C.; Pons, T.; Mertz, J.; Blanchard-Desce, M. *Tetrahedron Lett*. **2003**, *44*, 8121. (b) Venleton, L.; Moreaus, L.; Mertz, J.; Blanchard-Desce, M. *Chem. Commun.* **1999**, 2055.
(33) Lee, H. J.; Sohn, J.; Hwang, J.; Park, S. Y.; Choi, H.; Cha, M. *Chem. Mater*. **2004**, *16*, 456.
(34) Kogej, T.; Beljonne, D.; Meyers, F.; Perry, J. W.; Marder, S. R.; Bredas, J. L. *Chem. Phys. Lett.* **1998**, *298*, 1.
(35) Drobizhev, M.; Karotki, A.; Dzenis, Y.; Rebane, A.; Suo, Z.; Spangler, C. W. *J. Phys. Chem. B* **2003**, *107*, 7540.
(36) Jeong, H. C.; Piao, M. J.; Lee, S. H.; Jeong, M.-Y.; Kang, K. M.; Park, G.; Jeon, S.-J.; Cho, B. R. *Adv. Funct. Mater.* **2004**, *14*, 64.
(37) Varnavski, O. P.; Ostrowski, J. C.; Sukhomlinova, L.; Twieg, R. J.; Bazan, G. C.; Goodson, T., III. *J. Am. Chem. Soc.* **2002**, *124*, 1736.
(38) Katan, C.; Terenziani, F.; Mongin, O.; Werts, M. H. V.; Porrès, L.; Pons, T.; Mertz, J.; Tretiak, S.; Blanchard-Desce, M. *J. Phys. Chem. A* **2005**, *109*, 3024.
(39) Goodson, T., III. *Acc. Chem. Res*. **2005**, *38*, 99.
(40) Lahankar, A. S.; West, R.; Varnavski, O.; Xie, X.; Goodson, T., III; Sukhomlinova, L.; Twieg, R. *J. Chem. Phys.* **2004**, *120*, 337.
(41) Varnavski, O.; Samuel, I. D. W.; Palsson, L.-O.; Beavington, R.; Burn, P. L.; Goodson, T., III. *J. Chem. Phys.* **2002**, *116*, 8893.
(42) Wang, Y.; Ranasinghe, M. I.; Goodson, T., III. *J. Am. Chem. Soc.* **2003**, *125*, 9562.
(43) Varnavski, O.; Goodson, T., III; Sukhomlinova, L.; Twieg, R. *J. Phys. Chem. B* **2004**, *108*, 10484.
(44) Wang, Y.; He, G. S.; Prasad, P. N.; Goodson, T., III. *J. Am. Chem. Soc.* **2005**, *127*, 10128.
(45) Li, B.; Tong, R.; Zhu, R.; Meng, F.; Tian, H.; Qian, S. *J. Phys. Chem. B* **2005**, *109*, 10705.
(46) Goodson, T., III. *Annu. Rev. Phys. Chem.* **2005**. *56*, 581.
(47) Zhou, X.; Feng, J.; Ren, A. *Chem. Phys. Lett.* **2005**, *403*, 7.
(48) Drobizhev, M.; Rebane, A.; Suo, Z., Spangler, C. W. *J. Lumin.* **2005**, *111*, 291.
(49) Macak, P.; Luo, Y.; Norman, H.; Ågren, H. *J. Chem. Phys.* **2000**, *113*, 7055.
(50) Cho, B. R.; Son, K. H.; Lee, S. H.; Song, Y.-S.; Lee, Y.-K.; Jeon, S.-J.; Choi, J. H.; Lee, H.; Cho, M. *J. Am. Chem. Soc.* **2001**, *123*, 10039.
(51) Delgado, M. C. R.; Hernandez, V.; Casado, J.; Navarrete, J. T. L.; Raimudo, J.-M.; Blanchard, P.; Roncali, J. *Chem. Eur. J.* **2003**, *9*, 3670.
(52) Charlot, M.; Izard, N.; Mongin, O.; Riehl, D.; Blanchard-Desce, M.; *Chem. Phys. Lett.* **2006**, *417*, 297.
(53) Mongin, O.; Charlot, M.; Katan, C.; Porre;, L.; Parat, M.; Pions, T.; Mertz, J.; Blanchard-Desce, M. *Proc. SPIE Int. Soc. Opt. Eng.* **2004**, *9*, 5516.
(54) Cho, B. R.; Lee, S. J.; Lee, S. H.; Son, K. H.; Kim, Y. H.; Doo, J.-Y.; Lee, G. J.; Kang, T. I.; Lee, Y. K.; Cho, M.; Jeon, S.-J. *Chem. Mater.* **2001**, *13*, 1438.
(55) Cho, B. R.; Ratner, M. A.; Marks, T. J. *Chem. Rev.* **1994**, *94*, 195.
(56) McIlroy, S. P.; Clo, E.; Nikolajsen, L.; Federiksen, P. K.; Nielsen, C. B.; Mikkelsen, K. V.; Gothelf, K. V.; Ogilby, P. R. *J. Org. Chem.* **2005**, *70*, 1134.
(57) (a) Martin, R. E.; Diederich, F. *Angew. Chem., Int. Ed.* **1999**, *38*, 1350. (b) Lee, J. Y.; Kim, K. S.; Mhin, B. J. *J. Chem. Phys.* **2001**, *115*, 9484.

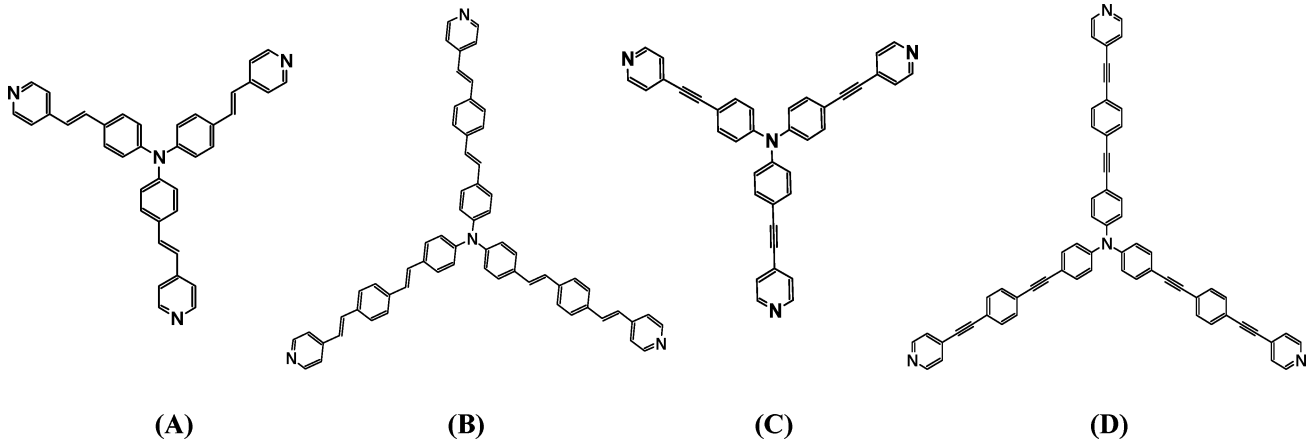

Figure 1. Chemical structures of the investigated chromophores.

Scheme 1. Synthesis of the Triply Branched Molecules **A**−**D**

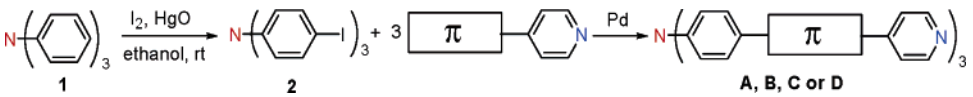

2. Experimental Details

2.1. Synthesis of Chromophores. ^{1}H NMR (300 MHz) and ^{13}C NMR (75 MHz) spectra were recorded with a Bruker AMX 300 spectrometer in $CDCl_3$ with tetramethylsilane as internal standard. Melting points were measured on a TA Instruments DSC 2920 instrument operating at 10 °C/min under nitrogen or by using a polarizing optical microscope equipped with a Mettler Toledo FP82HT heating stage attached to a Mettler Toledo FP90 temperature controller operating at 10 °C/min. High-resolution mass spectrometry (HRMS) was provided by the Mass Spec & Proteomics Facility at Ohio State University. The synthesis (Scheme 1) began with the iodination of triphenylamine **1** to afford tris(4-iodophenyl)amine **2** as a general central building block. The branches with alkene or alkyne conjugation and pyridine termini were synthesized as the π-building blocks. Finally, the triply branched molecules were synthesized by palladium-catalyzed coupling of **2** with the corresponding π-block fragment.

Tris[*p*-(4-pyridylvinyl)phenyl]amine (A). A mixture of tris(4-iodophenyl)amine (6.0 g, 9.63 mmol), 4-vinylpyridine (55.6 mmol), $Pd(OAc)_2$ (33 mg, 0.15 mmol), tri-*o*-tolylphosphine (93 mg, 0.3 mmol), triethylamine (10 mL), and acetonitrile (70 mL) was degassed with nitrogen. The reaction mixture was refluxed for 6 h. The mixture was cooled and poured into water. The precipitated orange solid was filtered off and washed with water. After drying under vacuum at 60 °C, the product was obtained as an orange solid (5.2 g, 97% yield). Mp: 266 °C (DSC). ^{1}H NMR ($CDCl_3$, 300 MHz): δ 8.56 (dd, J = 4.5, 1.5 Hz, 6H), 7.46 (d, 6H, J = 8.5 Hz), 7.35 (dd, J = 4.5, 1.5 Hz, 6H) 7.27 (d, J = 16.0 Hz, 3H), 7.14 (d, J = 8.5, 6H), 6.93 (d, J = 16.0, 3H). ^{13}C NMR ($CDCl_3$, 75 MHz): δ 150.3, 147.5, 144.9, 132.5, 131.5, 128.3, 125.0, 124.5, 120.8. HRMS (ES): m/z (M + H) calcd for $C_{39}H_{30}N_4$, 555.2470; found, 555.2505.

Tris((*E*)-2-{4-[(*E*)-2-pyridin-4-ylvinyl]phenyl}vinylphenyl)-amine (B). A mixture of tris(4-iodophenyl)amine (1.87 g, 3.0 mmol), 4-[4-ethenyl-(2-(*E*)-phenylethenyl)]pyridine (2.24 g, 10.8 mmol), $Pd(OAc)_2$ (44.8 mg, 0.2 mmol), triphenylphosphine (105 mg, 0.4 mmol), dimethylformamide (DMF) (50 mL), and triethylamine (20 mL) was degassed with nitrogen. The reaction mixture was heated at 45−50 °C for 24 h, and then it was cooled and poured onto 1000 mL of water. The precipitated orange solid was filtered off and washed with water. The orange solid was stirred in 100 mL of acetonitrile at 60 °C for 0.5 h and filtered. The resulting crude product was recrystallized from hot pyridine. The product was obtained as red needle-like crystals (1.50 g, 58% yield). Mp: 325 °C (DSC). ^{1}H NMR ($CDCl_3$, 300 MHz): δ 8.57 (dd, J = 4.5, 1.5 Hz, 6H), 7.53 (s, 12H), 7.45 (d, J = 9.0 Hz, 6H), 7.37 (dd, J = 4.5, 1.5 Hz, 6H), 7.30 (d, J = 17.0 Hz, 3H), 7.14 (d, J = 16.0 Hz, 3H), 7.13 (d, J = 8.0 Hz, 6H), 7.03 (d, J = 16.0 Hz, 3H), 7.02 (d, J = 16.0 Hz, 3H). ^{13}C NMR ($CDCl_3$, 75 MHz): δ 150.3, 147.0, 144.9, 138.2, 135.3, 132.9, 132.3, 128.8, 127.8, 127.6, 126.9, 125.8, 124.5, 121.0. Anal. Calcd for $C_{63}H_{48}N_4$: C, 87.87; H, 5.62; N, 6.51. Found: C, 87.48; H, 6.12; N, 6.66. HRMS (ES): m/z (M + H) calcd for $C_{63}H_{48}N_4$, 861.3957; found, 861.3964.

Tris[*p*-(4-pyridylethynyl)phenyl]amine (C). A mixture of tris(4-iodophenyl)amine (1.87 g, 3.0 mmol), 4-ethynylpyridine (1.12 g, 10.8 mmol), DMF (20 mL), triethylamine (10 mL), $Pd(PPh_3)_2Cl_2$ (56 mg, 0.080 mmol), PPh_3 (20 mg, 0.076 mmol), and CuI (16 mg, 0.084 mmol) was thoroughly degassed with nitrogen. The reaction mixture was stirred at 45 °C for 4 h. All the volatiles were removed under reduced pressure, and the residue was dissolved in 150 mL of CH_2Cl_2, washed with saturated aqueous Na_2CO_3 solution, dried over anhydrous Na_2SO_4, and filtered. The crude product was preloaded on silica gel and separated by flash column chromatography, eluting with CH_2Cl_2/EtOAc (up to 1:1). The product was obtained as light yellow needle-like crystals and was recrystallized from ethanol to give the product as yellow crystals (1.05 g, 64% yield). Mp: 203 °C. ^{1}H NMR (300 MHz, $CDCl_3$): δ 8.59 (dd, J = 4.8, 1.2 Hz, 6H), 7.47 (ddd, J = 9.0, 2.1, 2.1 Hz, 6H), 7.35 (dd, J = 4.8, 1.2 Hz, 6H), 7.10 (ddd, J = 9.0, 2.1, 2.1 Hz, 6H). ^{13}C NMR (75 MHz, $CDCl_3$): δ 149.9, 147.3, 133.4, 131.6, 125.6, 124.3, 117.2, 93.9, 87.0. HRMS (ES): m/z (M + H) calcd for $C_{39}H_{24}N_4$, 549.2079; found, 549.2072.

Tris{*p*-[4-pyridylethynyl(4-phenylethynyl)]phenyl}amine (D). A mixture of tris(4-iodophenyl)amine (1.25 g, 2.0 mmol), 4-(4-ethynyl-phenylethyl)pyridine (1.46 g, 7.2 mmol), DMF (30 mL), triethylamine (10 mL), $Pd(PPh_3)_2Cl_2$ (56 mg, 0.080 mmol), PPh_3 (20 mg, 0.076 mmol), and CuI (16 mg, 0.084 mmol) was thoroughly degassed with nitrogen. The reaction mixture was stirred at 55 °C for 8 h. A blue fluorescence was observed from the reaction mixture. All the volatiles were removed under reduced pressure, and the residue was dissolved in 200 mL of CH_2Cl_2, washed with saturated aqueous Na_2CO_3 solution, and dried over anhydrous Na_2SO_4. This crude product was preloaded on silica gel and separated by flash column chromatography, eluting with CH_2Cl_2/EtOAc (1:1), and finally up to 5% MeOH was added to elute the product. This product was further purified by recrystallization from pyridine to give the product as yellow crystals (0.87 g, 51%). Mp: 225 and 241 °C (DSC). ^{1}H NMR (300 MHz, $CDCl_3$): δ 8.61 (dd, J = 4.5, 1.5 Hz, 6H), 7.52 (s, 12H), 7.45 (d, J = 8.7 Hz, 6H), 7.38 (dd, J = 4.5, 1.5 Hz, 6H), 7.09 (d, J = 8.7 Hz, 6H). ^{13}C NMR (75

MHz, $CDCl_3$): δ 150.0, 147.0, 133.1, 132.0, 131.7, 131.4, 125.7, 124.4, 124.3, 121.8, 117.8, 93.8, 91.9, 89.1, 88.5. HRMS (ES): m/z (M + H) calcd for $C_{63}H_{36}N_4$, 849.3018; found, 849.2969.

2.2. Steady-State Measurements. All compounds were used as received without any further purification. They were dissolved in tetrahydrofuran (THF) (Sigma-Aldrich, spectrophotometric grade). The absorption spectra of the molecules were measured using an Agilent model 8341 spectrophotometer. To measure molar extinction coefficients, the original stock solutions were diluted to 10^{-6} M. The emission spectra were acquired using a Shimadzu RF-1501 instrument. The quantum yields of the molecules were measured using a known procedure.[58] Coumarin 307 was used as the standard. The absorbance was limited to equal to or less than 0.03. The solutions were purged with argon for 3 min prior to measuring their emission spectra. The following relation was then used to measure the quantum yield:

$$\phi_F = (\phi_F)_S \frac{\int J(\bar{\nu})\, d\bar{\nu}}{\int J_S(\bar{\nu})\, d\bar{\nu}} \frac{(J_a)_S}{J_a} \frac{n^2}{n_s^2} \quad (1)$$

These measurements may have some error due to the sensitivity of the fluorescence spectrophotometer and other environmental conditions.

2.3. Two-Photon Excited Fluorescence Measurements. To measure the 2PA cross sections, we followed the two-photon excited fluorescence (TPEF) method.[59] A 10^{-4} M solution of Coumarin 307 in methanol was used as the reference. The laser used for the study was a Kapteyn Murnane (KM) mode-locked Ti:sapphire laser. The bandwidth at 800 nm was 47 nm, and the pulse duration was ~30 fs. The input power from the laser was varied by using a polarizer. An iris was placed prior to the polarizer in order to ensure a circular beam. The beam from the polarizer was focused on the sample cell (quartz cuvette, 0.5 cm path length) using a lens with a focal length of 11.5 cm. The fluorescence was collected in a direction perpendicular to the incident beam. A 1-in. focal length planoconvex lens was used to direct the collected fluorescence into a monochromator. The output from the monochromator was coupled to a photomultiplier tube. The photons were converted into counts by a photon counting unit. A logarithmic plot between collected fluorescence photons and input intensity gave a slope of 2, ensuring a quadratic dependence between the same. The intercept enabled us to calculate the 2PA cross section.

2.4. Non-degenerate Two-Photon Absorption Measurements. In addition to the degenerate 2PA cross sections taken at discrete wavelengths described above, the full non-degenerate 2PA spectra of the molecules were also obtained.[60] The femtosecond laser system employed was a CPA-2001 (CLARK-MXR) amplified Ti:sapphire system operating at 775 nm with ~0.9 mJ/pulse, 140 fs pulses at a 1 kHz repetition rate. This laser in turn pumped two widely tunable optical parametric amplifiers (TOPAS, Light Conversion Ltd.). In this experiment, a strong (high irradiance) pump beam from TOPAS1 induced the nonlinearity in the sample and a weak probe beam from TOPAS2 monitored that nonlinearity. To be able to measure a wide spectral range of the 2PA spectrum, the probe beam used was a very broadband white-light continuum (WLC) pulse (400−1700 nm) produced by focusing 1−2 μJ into a 2.5 mm thick piece of calcium fluoride. The two pulses, pump and probe, were overlapped in both space and time on the sample under investigation. In this non-degenerate experiment, one photon from the pump and one photon from the probe (within the broadband WLC) were simultaneously absorbed. By monitoring the transmission of the broadband WLC probe using a dual-fiber input spectrometer (Acton Spectro150) that was coupled to a dual-diode array (Princeton Instruments DPDA 2048), we could ascertain the strength of the 2PA versus wavelength or equivalently the 2PA spectrum.

The pump wavelength was set to 1200 nm when acquiring the nonlinear absorption spectra to avoid any degenerate 2PA of the pump itself. This was done for the purpose of avoiding any spurious excited-state absorption following 2PA of the pump beam itself. The non-degenerate spectra will exhibit larger 2PA cross sections than those found by degenerate excitation due to pre-resonance enhancement effects.[61] The magnitude of this enhancement is determined by the photon energies of the pump and probe and the transition energies of the one- and two-photon allowed states. An enhancement factor (for non-degenerate excitation) was obtained by use of eq 2 in ref 61, as well as from the transition energies of the lowest-lying one-photon allowed states and the energies of the higher-lying two-photon allowed states. Although this factor did show some dispersion over the region of interest (i.e., 380−450 nm), the effect is small and the factor was found to be approximately 2.0 over this range. Therefore, non-degenerate excitation will exhibit a 2 times higher strength of 2PA compared to degenerate excitation. The values of the non-degenerate cross sections, discussed later, have been scaled by this factor to allow a more direct comparison with the values of the degenerate 2PA cross sections.

2.5. Fluorescence Lifetime Measurements. Time-correlated single photon counting (TCSPC) was performed to determine the fluorescence lifetimes of the molecules. Along with their quantum yields, their radiative lifetimes could be determined. The laser used was the same as for TPEF measurements. The 800 nm output was frequency-doubled using a BBO crystal.

2.6. Ultrafast Transient Absorption Measurements. Femtosecond transient absorption investigations were carried out using an ultrafast pump−probe spectrometer detecting in the visible region. Briefly, 1 mJ, 100 fs pulses at 800 nm with a repetition rate of 1 kHz were obtained from a Nd:YLF (Empower)-pumped Ti:sapphire regenerative amplifier (Spitfire, Spectra Physics), with the seed pulses from a Millennia-pumped Ti:sapphire oscillator (Tsunami, Spectra Physics). The output of the laser beam was split to generate pump and probe beam pulses with a beam splitter (85% and 15%). The pump beam was produced by an optical parametric amplifier (OPA-800). The pump beam used in the present investigation, i.e., 420 nm, was obtained from the fourth harmonic of the idler beam and was focused onto the sample cuvette. The probe beam was delayed with a computer-controlled motion controller and then focused onto a 2 mm sapphire plate to generate a white light continuum. The white light was then overlapped with the pump beam in a 2 mm quartz cuvette containing the sample, and the change in absorbance for the signal was collected by a CCD detector (Ocean Optics). Data acquisition was controlled by software from Ultrafast Systems Inc. Typical energy of the probe beam was <0.1 μJ, while that of the pump beam was around 0.5−1 μJ per pulse. Magic angle polarization was maintained between the pump and probe using a wave plate. The pulse duration was obtained from fitting of the solvent response, which was ~130 fs. The sample was stirred by a rotating magnetic stirrer.

3. Results and Discussion

3.1. Optical Absorption and Steady-State Fluorescence Measurements. The linear and nonlinear optical properties of all the branched systems are summarized in Table 1. The optical absorption and emission characteristics of compounds **A**−**D** in THF are shown in Figure 2. One notes the expected shift in the absorption maximum to longer wavelengths on going from **A** to **B** and from **C** to **D** due to increases in conjugation length. Also, the absorption maxima of alkyne π-bridged compounds are blue-shifted relative to their alkene counterparts. This is because, in the alkene chromophores, all the carbon atoms on

(58) Maciejewski, A.; Steer, R. P. *J. Photochem.* **1986**, *35*, 59.
(59) Xu, C.; Webb, W. W. *J. Opt. Soc. Am. B* **1996**, *13*, 481.
(60) Negres, R. A.; Hales, J. M.; Kobyakov, A.; Hagan, D. J.; Van Stryland, E. W. *IEEE J. Quantum Electron.* **2002**, *38*, 1205.
(61) Hales, J. M.; Hagan, D. J.; Van Stryland, E. W.; Schafer, K. J.; Morales, A. R.; Belfield, K. D.; Pacher, P.; Kwon, O.; Zojer, E.; Bredas, J. L. *J. Chem. Phys.* **2004**, *121*, 3152.

Table 1. Summary of Linear and Nonlinear Optical Properties of the Chromophores

molecule	λ_{abs} (nm)	λ_{em} (nm)	δ (GM)	η	τ_r (ns)	μ (D)
A	406	479	370[a] (187)	0.23	10	3.3
B	426	519	1037[a] (812)	0.26	8	3.9
C	377	428	91[b] (102)	0.58	2.7	5.6
D	391	455	280[a] (283)	0.55	2.7	5.8
$N(DSB)_3$	419	484	270[a]	0.48	3	5.9
PRL-701	422	502	491[a]	0.51	2.9	5.5

[a] 800 nm excitation. [b] 770 nm excitation. Values in parentheses are from non-degenerate pump−probe measurements. λ_{abs} and λ_{em} are absorption and emission maxima, respectively; δ is the 2PA cross section; η is the fluorescence quantum yield; τ_r is the radiative lifetime; and μ is the emission transition dipole moment calculated from the Strickler−Berg formula.[64]

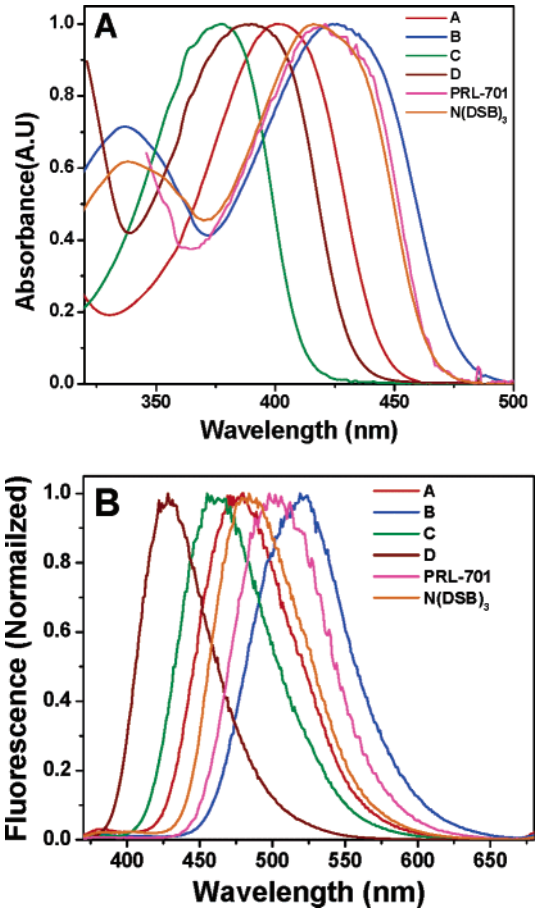

Figure 2. (A) Absorption spectra and (B) Fluorescence spectra of investigated branched molecules.

the branches are sp^2 hybridized. However, in the case of the alkyne chromophores, the carbon atoms are both sp and sp^2 hybridized. This results in poorer π-orbital overlap and mismatch in energies of the π-orbitals.[62,63] It should also be noted from Table 1 that, as the acceptor group strength increases (from *tert*-butylbenzene to dioxazole to pyridine), the Stokes shift increases (4206 cm^{-1} for the alkene system **B** is higher than for the two previously reported nitrogen-centered chromophores, $N(DSB)_3$ and PRL-701,[44] where the pyridine group is replaced by *tert*-butyl and oxadiazole groups, respectively). The increase in Stokes shift can be attributed to increase in charge-transfer character of the respective chromophores. For the molecules

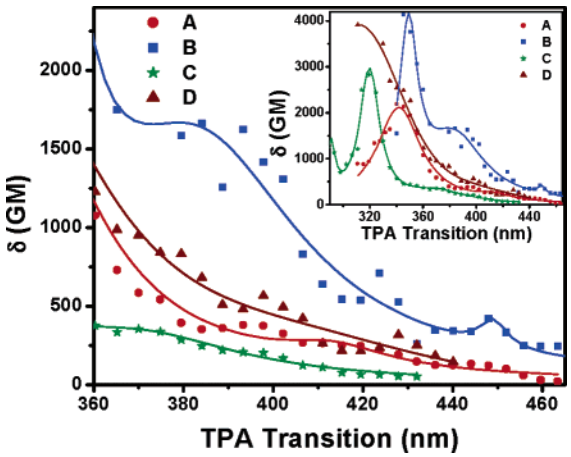

Figure 3. Non-degenerate 2PA spectra of the molecules in the region of low-energy absorption band. Inset shows the entire spectrum. The lines are shown as guides for the eye.

with same acceptors, alkene π-bridged chromophores are found to have higher Stokes shifts than alkyne π-bridged chromophores.

Fluorescence quantum yield and fluorescence lifetimes (with time-correlated single photon counting) have been determined for all the molecules. The alkyne π-bridged chromophores showed approximately twice the quantum yield as their alkene counterparts (Table 1). From the lifetimes of the excited states, radiative lifetimes and emission transition dipole moments (μ) have been determined and are provided in Table 1. It can be noted from the table that the alkene π-bridged chromophores **A** and **B** have lower μ than their alkyne counterparts **C** and **D**. It is also noteworthy that conjugation length does not have a significant impact on the radiative lifetime of these chromophores. On the basis of the optical absorption measurements (extinction coefficient and area under the absorption curve), the absorption transition dipole moments (M_{ge}) have also been calculated. An increase in the conjugation length is found to increase the M_{ge}. The acceptor strength does not seem to play a major role in determining M_{ge}, while it does have a significant impact on the Stokes shifts. On the basis of the absorption and emission transition dipole moments calculated from steady-state measurements, it appears that the alkyne π-bridged branched chromophores would have greater 2PA cross sections than their alkene analogues. On the other hand, the trend observed from Stokes shift measurements shows that the alkene π-bridged chromophores would have higher 2PA cross sections than their alkyne counterparts. This suggests that steady-state measurements alone cannot explain the trends observed in branched chromophore systems, and time-resolved techniques should be employed (see below).

3.2. Two-Photon Absorption Cross-Section Measurements. Two-photon absorption cross-section measurements have been carried out using two-photon excited fluorescence (TPEF) as well as with non-degenerate 2PA setup. Figure 3 shows the 2PA cross-section spectrum for chromophores **A**−**D**, where the cross sections are plotted versus the transition energy expressed in wavelength. As a comparison, the cross sections at 770 or 800 nm (at the maximum of the lowest-energy absorption band) for the molecules are listed in Table 1 as well (shown in parentheses are the non-degenerate 2PA cross sections at those wavelengths). It is worth reiterating that non-degenerate 2PA has shown larger

(62) Dewar, M. J. S. *J. Am. Chem. Soc.* **1952**, *72*, 1345.
(63) Cheng, L.; Tam, W.; Marder, S. R.; Stiegman, A. E.; Rikken, G.; Spangler, C. W. *J. Phys. Chem.* **1991**, *95*, 10643.

than 2PA at equivalent values for degenerate excitation. For this reason, the values in Table 1 have been reduced by an appropriate scaling factor to make a more direct comparison with the degenerate 2PA cross sections.[61]

There are several comparisons that can be made regarding the 2PA properties observed in these systems. First, a comparison between the linear and nonlinear absorption spectra reveals that all the molecules exhibit substantial 2PA into the lowest-energy absorption band (i.e., 380−450 nm), which is both one- and two-photon allowed.[29] There also exists a stronger, higher-energy two-photon-allowed state which lies between the two one-photon bands (inset of Figure 3), which has been attributed to strong electronic coupling between the branches. Furthermore, the trends observed for both the degenerate and non-degenerate cross sections in Table 1 are quite similar. The two alkene-containing systems (**A** and **B**) differ only by an increase in the conjugation length of the individual arm by one vinylene unit. In the lowest-energy absorption band, one observes a 3-fold increase in 2PA cross section for **B** in comparison to **A**. The same trends can be noted for compounds **C** and **D**, which both contain alkynes. This effect of increasing conjugation on 2PA cross section has been well documented in the literature.[64,65] An increase in conjugation reduces the detuning term (the energy difference between the ground and first excited states and the ground and 2PA states) in the sum-over-states expression[29] and also increases the transition dipole moment. As a result of these two contributions, the 2PA cross section increases significantly. Comparing chromophores **B** and **D**, which contain similar chromophore density, it is clearly seen that the 2PA of the alkene branched system **B** is approximately 3.7 times higher than that of its alkyne counterpart **D**. Similarly, the ratio of 2PA cross sections between **A** and **C** is 4. A direct comparison between molecular systems can be made by normalizing the cross sections listed in Table 1 to their respective molecular weights. Still, the alkene chromophores show a 4-fold increase in 2PA cross section when compared to the corresponding alkynes at the low-energy peak.

The influence of acceptor strength is also seen from the results presented in Table 1. As the acceptor unit is changed from *tert*-butylbenzene to oxadiazole in $N(DSB)_3$ to PRL-701, respectively, we see a substantial increase in 2PA cross section. This effect is more pronounced when a stronger acceptor, namely pyridine, is introduced in molecule **A**. The argument that acceptor strength increases from *tert*-butylbenzene to pyridine can be verified from their Hammett constants.[67] Chromophore **A** has 4 times higher δ than $N(DSB)_3$. These observations can be attributed to increased acceptor strength, which imparts a higher amount of charge-transfer character. It has been shown theoretically by Cho et al.[49] that the 2PA cross section increases with an increase in donor or acceptor strength. The measurements presented here show that the extent of charge-transfer character is important in increasing the 2PA cross section.

A surprising trend is observed when considering the high-energy 2PA band shown in the inset of Figure 3. When we compare **A** and **B**, there is an increase in the 2PA cross section by a factor of 2, and the increase is a factor of about 1.5 when **C** and **D** are compared, suggesting the effect of conjugation length. As the conjugation length is increased, the absorption transition dipole moment is increased (Table 1) and the detuning factor is decreased, thereby influencing the 2PA cross section. It is interesting to see the trend observed in the cross section for 2PA to high-energy states for alkene and alkyne π-bridging branched chromophores. When we compare **A** and **C**, the alkyne π-bridged chromophore's (**C**) cross section is around 1.4 times higher than that of the corresponding alkene analogue (**A**). As mentioned above, the expected trend in transition moments suggests that the 2PA in the alkene systems is longer. This is contrary to what the steady-state results predicted. However, ultrafast time-resolved measurements, which give information about excited-state characteristics, are able to probe these differences. It is to be noted here that, when cross sections for 2PA to higher-energy states are concerned, it involves knowledge of the excited-state transition dipole moment (from the sum-over-states formalism). Estimates of excited-state transition dipole moment can be obtained from ultrafast transient absorption measurements.

3.4. Transient Absorption Measurements. Among all the investigated trimers, trimer **B** showed the largest 2PA cross section in comparison to the other chromophores. By changing the bridging unit from alkyne to alkene, there is a substantial increase in 2PA cross section, which also increases with an increase in acceptor strength. Thus, it is evident that the charge-transfer character of the molecules does play an important role in determining the 2PA cross section of the molecules. Steady-state measurements based on absorption, emission transition dipole moments, and Stokes shift were unable to provide a conclusive explanation for the observed differences in the 2PA cross section of alkene and alkyne π-bridging molecules as well as branched molecules with increase in acceptor strength. Thus, we evaluated the extent of charge transfer in the excited state as well as excited-state transition dipole moments by ultrafast pump−probe measurements. To illustrate the importance of the extent of intramolecular charge transfer (ICT) in the excited state immediately after photoexcitation with regard to the 2PA cross sections, ultrafast transient absorption measurements of molecules **A**−**D** were carried out. Shown in Figure 4A are the transient absorption spectra at different time delays (from 150 fs to 26 ps) of trimer **B** in THF. At the time delay of 150 fs, a bleach in the region of 450−540 nm and a positive transient absorption greater than 540 nm are observed. The bleach centered at ~470 nm can be ascribed to the stimulated emission from the ICT state of the trimer. The positive absorption is attributed to the excited-state absorption (ESA) arising from the ICT state.

The observation of stimulated emission and ESA from the ICT state at a time delay of 150 fs suggests that the internal conversion from the initially populated C_3-symmetry state to the charge-localized ICT state happens much faster than 100 fs, which indicates that the Franck−Condon (FC) state and the ICT state are intimately linked by the same reaction coordinate. However, as the time delay is increased to 26 ps, a new transient started to grow in the region of 460−540 nm with a decay of ESA of the ICT state. Population of this transient was found to increase with increasing polarity of the solvents and strength of donor−acceptors. Thus, this ESA is ascribed to the solvent and the conformationally stabilized ICT state (ICT′ state). It is

(64) Strickler, S. J.; Berg, R. A. *J. Chem. Phys.* **1962**, *37*, 814.
(65) Rubio-Pions, O.; Luo, Y.; Agren, H. *J. Chem. Phys.* **2006**, *124*, 094310.
(66) Ray, P. C.; Leszczynski, J. *J. Phys. Chem. A* **2005**, *109*, 6689.
(67) Hansch, C.; Leo, A.; Taft, R. W. *Chem. Rev.* **1991**, *91*, 165.

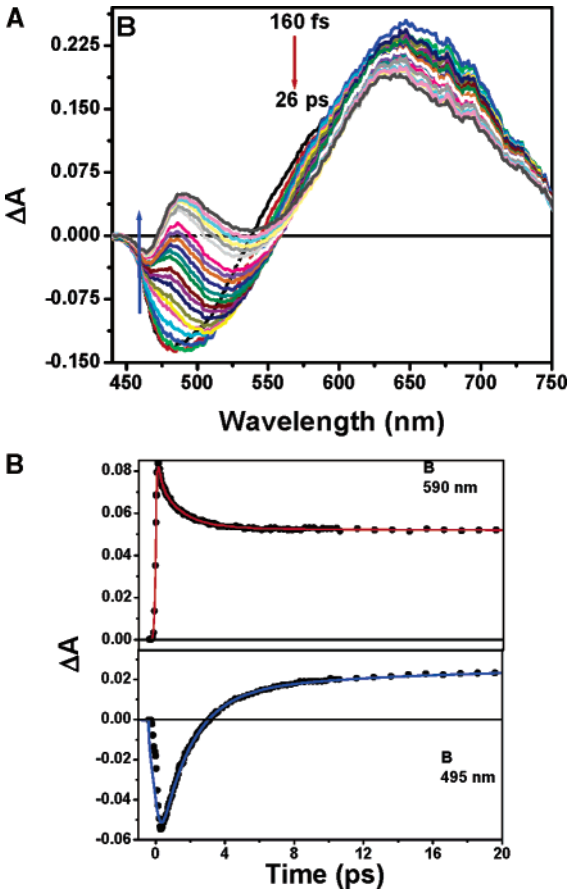

Figure 4. (A) Transient absorption spectra of **B** in THF at different time delays from 150 fs to 30 ps. (B) Kinetics at 590 and 495 nm.

to be noted here that the ICT′ state is not emissive and can be ascribed to a twisted intramolecular charge transfer ICT state. The kinetic traces shown in Figure 4B show that the decay of the ICT state matches the growth of the ICT′ state, and they constitute a predecessor−successor pair. Global fit analysis of all the decay traces has yielded two time constants of 2.8 ps and >1 ns. The time constant of 2.8 ps has been ascribed to the time scale of internal conversion from the ICT state to the ICT′ state, and a >1 ns time constant is ascribed to the excited-state lifetime.

Transient absorption measurements have also been carried out on trimer **D** dissolved in THF, and the corresponding transient absorption spectra are shown in Figure 5A. At the initial time delay, a bleach in the region of 450−500 nm and a positive absorption greater than 500 nm with a maximum around 560 nm are observed. The bleach has been ascribed to stimulated emission from the ICT and the positive absorption to ESA of the ICT state. Ultrafast charge localization from the FC state to the ICT state has also been observed here, suggesting that the FC and ICT states are linked by the same reaction coordinate.

Similar to what has been observed in the case of trimer **B**, formation of a new transient is observed as the time delay is increased to 30 ps, although the amplitude of the observed new transient is small. Evolutions of the transients are better viewed by following the kinetic decay traces at 450 and 590 nm, as shown in Figure 5B. The kinetics at 450 nm shows the presence of the new transient state, and its growth matches well with the decay of ESA at 590 nm. This new transient can be once again

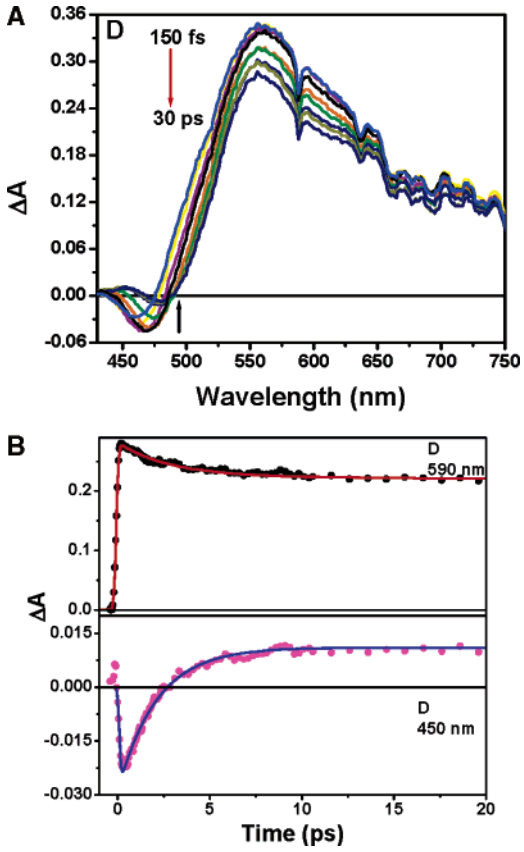

Figure 5. (A) Transient absorption spectra of **D** in THF at different time delays from 150 fs to 30 ps. (B) Kinetics of the transients at 590 and 450 nm.

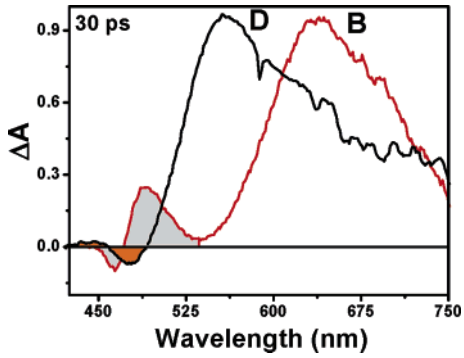

Figure 6. Comparison of the ICT′ states for trimers **D** and **B**. It can be observed that the population of ICT′ for **B** is higher than that for **D**.

attributed to ESA of the ICT′ state. Global fit analysis has yielded two time constants, 2.1 ps and >1 ns, similar to those observed in the case of **B**. However, it is interesting to note that the populations of this ICT′ state are different for **D** and **B**; the population is higher in the case of **B** over **D** in the same solvent.

As mentioned above, the population of the ICT′ state depends on the polarity of the solvent and the strength of the acceptor. Thus, it can be used as an indicator of the amount of charge transfer in the excited state of the trimers. Figure 6 shows the comparison of the populations of the ICT′ states for **B** and **D** in THF at a time delay of 30 ps. Under similar solvent polarity, the population of the ICT′ state can be directly ascribed to the degree of charge-transfer character. It can be observed from Figure 6 that the amplitude of ICT′ for the alkene branched

system **B** is much higher in comparison to that for the alkyne branched system **D** in the same solvent. This result suggests that the amount of charge transfer in the case of **B** is larger than that in **D**. As the 2PA cross section mainly concerns the FC state, knowledge of the amount of charge transfer concerning the FC state is needed. The FC and ICT states are intimately linked by the same reaction coordinate by virtue of ultrafast charge localization from the FC to the ICT state. Hence, one can extrapolate the extent of charge transfer observed in the ICT state to the FC state.[68,69] The results thus confirm that the extent of CT in the alkene branched system **B** is higher than that in **D**, and therefore **B** displays a higher 2PA cross section. The result of a larger δ for **B** in comparison to **D** was somewhat surprising, as one also notes the increase in quantum yield and calculated transition dipole moments for the alkyne system. However, the magnitude of δ in the alkyne π-system **D** is significantly smaller than that observed for the alkene π-system **B**, and this mainly is related to the increased CT character and stronger delocalization. This conclusion is obtained from time-resolved absorption measurements, as the steady-state measurements favor a larger cross section for **D** than for **B**.

Another important aspect that has been observed in 2PA cross-section measurements is that, as the acceptor strength is increased, the 2PA cross section is increased. This can be mainly ascribed to the CT of both ground and excited states. It is well known that higher acceptor strength results in a greater degree of charge transfer in a donor−acceptor type system, which thereby shows higher NLO properties. It has been demonstrated earlier in this section that the extent of CT in the excited state can be monitored by femtosecond pump−probe spectroscopic results. Similar transient absorption measurements have been carried out to understand the effect of acceptor strength on 2PA cross section. Shown in Figure 7 are the transient absorption spectra of PRL-701 and $N(DSB)_3$ in acetonitrile (3D representation of the ESA spectra), in which PRL-701 has shown a larger 2PA cross section by virtue of its larger acceptor strength. Upon comparing $N(DSB)_3$ and PRL-701, with PRL-701 having the stronger acceptor in the oxadiazole molecule, it is clearly seen that the ratio of ICT′:ICT population is greater in the case of PRL-701, suggesting that the amount of CT in the case of PRL-701 is obviously higher than that in $N(DSB)_3$.

Estimates of excited-state extinction coefficients have also been made for the chromophores **B** and **D** under actinometric conditions by ultrafast transient absorption spectroscopy. It has been observed from our transient measurements that the excited-state extinction coefficient of chromophore **B** is about 2 times larger than that of **D**. Using the excited-state extinction coefficients and the area under the curve of the ESA spectrum, we have determined the excited-state transition dipole moment. It is found to be around 1.5 times higher for alkyne branched chromophore **D** in comparison to alkene branched chromophore **B**. The higher excited-state transition dipole moment contributes mainly to the 2PA into the higher-energy two-photon absorption bands.

3.5. Factors and Rationale for Influencing the Two-Photon Absorption Cross Section in Branched Systems. As mentioned in the Introduction, several parameters influence the

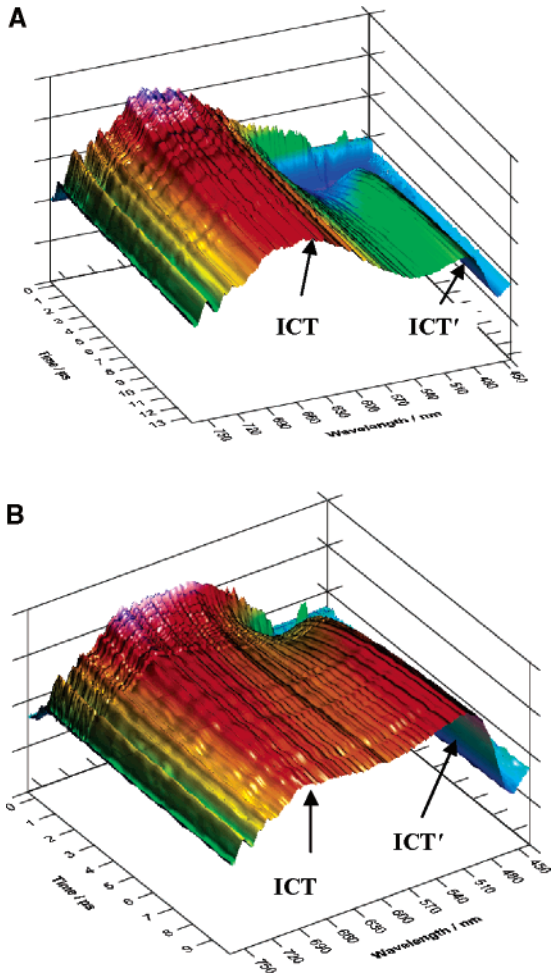

Figure 7. Comparison of the ICT′ states' populations for molecules $N(DSB)_3$ and PRL-701 in acetonitrile. It can be observed that ICT′:ICT is higher for PRL-701.

effective 2PA cross sections of molecules. Within the framework of the sum-over-states model,[29] the cross section for 2PA into the lowest-energy absorption band for non-centrosymmetric molecules can be expressed as

$$\delta_{2-\text{state}} \propto \frac{M_{ge''}{}^2 \, \Delta\mu_{ge'}{}^2}{\Gamma} \tag{2}$$

and that for 2PA into high-lying states that are not dipole coupled to the ground state can be written as

$$\delta_{2-\text{state}} \propto \frac{M_{ge''}{}^2 \, M_{ee'}{}^2}{(E_{ge} - E_{ge'}/2)^2 \Gamma} \tag{3}$$

Here, M_{ge} and $M_{ge'}$ are the transition dipole moments from the ground state to excited states e and e′, respectively; E_{ge} and $E_{ge'}$ are the corresponding transition energies from the ground state to the e and e′ states, respectively; and Γ is the damping factor. Equation 2 is the dipolar term while eq 3 is the two-photon term in the complete sum-over-states model. Under this model, the cross section for 2PA to the low-lying excited state of chromophores containing charge-transfer states is mainly controlled by three important parameters: the excitation energy, the oscillator strength, and the change in dipole moment related to the low-lying CT state.[29] For the higher-energy 2PA states,

(68) Ramakrishna, G.; Goodson, T. G., III, submitted for publication.
(69) Premvardhan, L.; Papagiannakis, E.; Hiller, R. G.; van Gorndelle, R. *J. Phys. Chem. B* **2005**, *109*, 15589.

along with these parameters the cross section for 2PA is also controlled by the excited-state transition dipole moment. The present 2PA cross-section measurements of triphenylamine-core branched molecules have displayed some interesting magnitudes of 2PA cross section with respect to the nature of the substituents.

Effect of Conjugation Length. The two alkene π-bridge-containing systems (**A** and **B**) differ in the conjugation length of the ligand, and concurrently one observes about a 3-fold increase in the cross section for **B** in comparison to that for **A**. The same trend can be noted for compounds **C** and **D**, both containing alkyne π-bridges. It can be observed from Table 1 that, as the conjugation length is increased, there is a clear red shift in the optical absorption and emission for both alkene and alkyne π-bridging molecules. The Stokes shift is also increased with increase in conjugation length, indicating an increase in effective conjugation length. All these parameters result in increases of the oscillator strength of the absorption band[66,67] and the transition dipole moment of the absorption. Also, the shift of absorption to longer wavelengths with an increase in conjugation decreases the detuning energy present in the two-photon term (eq 3), thereby enhancing the 2PA cross section.

Effect of Acceptor Strength. With increasing the acceptor strength from $N(DSB)_3$ to PRL-701 to **B**, there is and enhancement in the 2PA cross section. Unlike the quadrupolar molecules, where the one-photon-allowed states are not two-photon allowed, in multiply branched chromophores, the low-lying states are both one- and two-photon allowed. In such a situation, one-photon photophysics and excited-state deactivation can be correlated with the observed 2PA cross sections. Although enhancement of the 2PA cross sections through substitution with electron-withdrawing and electron-donating groups is well established both experimentally and theoretically, the electronic origin of the enhancement is not yet fully understood.[29] In the present investigation, through our transient absorption measurements, we have shown that, as the acceptor strength is increased, the extent of charge transfer in the FC state is increasing, which cannot be understood on the basis of steady-state measurements alone. This will result in a net change in the dipole moment and significantly contribute to the dipole term in the 2PA cross section, thereby increasing the 2PA cross section with increase in acceptor strength.

Effect of π-Bridging. It has been shown in the literature that, in donor−bridge−acceptor molecules, the lowest-energy ICT state is influenced not only by the donor−acceptor strength but also by the bridge and substituents.[70] In the present investigation, a direct comparison between molecular systems can be made by normalizing the cross sections listed in Table 1 to their respective number of π-electrons. In this case, alkene π-bridge-containing molecules **A** and **B** exhibit larger normalized 2PA values (by 4.4 and 4.0 times, respectively) than their alkyne π-bridged counterparts of **C** and **D**. One also notes from Table 1 that, within the two respective systems (alkene and alkyne), there is no significant change in the transition dipole moment. Transient absorption measurements carried out for alkene and alkyne π-bridged chromophores **B** and **D** have shown a higher population of the ICT′ state for **B** over **D**, which indicates that the extent of charge transfer in the ICT state of **B** is higher than in **D**. It has also been observed that there is ultrafast charge localization from the FC state to the ICT state, indicating that the two states are intimately connected by the same reaction coordinate. Thus, the amount of CT in the ICT state is correlated to the FC state, which indicates that the extent of charge transfer is higher for alkene π-bridged chromophores in comparison to the alkyne π-bridged chromophores. This will contribute significantly to the net change in dipole moment of the molecule and to the dipole term of 2PA (eq 2, 2PA into the one-photon-allowed CT state). This explains the higher cross section observed for alkene π-bridged chromophores over alkyne π-bridged chromophores for the low-energy peak.

However, 2PA into high-energy 2PA states involves the summation of eqs 2 and 3. From transient absorption spectroscopy, two important results are obtained with regard to alkene and alkyne π-bridged chromophores. The extent of charge transfer, which contributes mainly to the low-lying 2PA effect band, is higher for alkene π-bridged chromophores than for the alkyne analogues, while the estimates of excited-state transition dipole moment favor the alkyne π-bridged chromophores over the alkene analogues. These two terms contribute in opposite directions, and their summation gives almost equal cross sections for 2PA into higher-energy 2PA bands for both **B** and **D**. This stresses very strongly the need for the use of combined techniques (TPEF, non-degenerate pump−probe, ultrafast transient absorption spectroscopy) to evaluate the differences in observed 2PA cross section. Actually, this is a novel approach in which different 2PA techniques as well as steady-state and time-resolved measurements are all used to unravel the mechanism of the 2PA cross section. The extent of charge transfer in the excited state has been clearly evaluated, and one finds that this approach is more in-depth than the measurements of the cross section alone.

4. Conclusions

In conclusion, we have synthesized a set of triphenylamine-centered branched structures with pyridine acceptor groups to investigate their two-photon absorption and photophysical properties and compared them with previously reported branched chromophores. Two-photon absorption measurements have shown that increases in conjugation length and acceptor strength enhance the cross section, while the alkene π-bridged branched chromophores show significantly higher 2PA cross section than the alkyne π-bridged chromophores, especially in the region of the low-energy absorption band. The Stokes shift and emission transition dipole moments determined from steady-state and fluorescence lifetime measurements are not sufficient to predict the trends observed in 2PA cross sections. The results indicate that charge transfer in the excited state plays a vital role in increasing the 2PA cross section. Ultrafast transient absorption spectroscopy was used to measure the amount of charge transfer in the excited state. It has been shown that alkene π-bridged systems possess a greater amount of charge transfer by virtue of a greater population of the ICT′ state, and this is the reason for the increased 2PA cross section in these chromophores. Estimates of excited-state transition dipole moments have explained the observed differences in 2PA in high-energy 2PA states. These trends were not predicted by steady-state measurements; the combined approach allows one to probe the mechanism of 2PA in branched structures closely. Overall, the most

(70) Ahlheim, M.; Barzoukas, M.; Bedworth, P. V.; Blanchard-Desce, M.; Fort, A.; Hu, Z.-Y.; Marder, S. R.; Perry, J. W.; Runser, C.; Statehelin, M.; Zysset, B. *Science* **1996**, *271*, 335.

extended alkene π-bridged system showed the largest 2PA cross section at the low-energy peak for reasons related to increased conjugation length and larger CT character. These results suggest that alkene and alkyne π-extended systems with acceptors such as pyridine have better 2PA properties, and they would serve as good building blocks for larger branched systems.

Acknowledgment. T.G. acknowledges the Army Research Office and the National Science Foundation for support. J.M.H. acknowledges the Army Research Labs and the National Science Foundation for support.

Supporting Information Available: Complete refs 1a,b. This material is available free of charge via the Internet at http://pubs.acs.org.

JA060630M